Journal of Earth Sciences and Geotechnical Engineering, Vol.9, No. 3, 2019, 101-116
ISSN: 1792-9040 (print version), 1792-9660 (online)
Scientific Press International Limited

Micro- and macroscopic ion diffusion controlled by clay micro-structure

Roland Pusch[1] and Viktor Popov[2]

Abstract

Very dense smectite clay surrounding canisters with high-level radioactive waste effectively stops migration of radionuclides due to flowing porewater, however, does not stop their movement by diffusion. The paper explains how the diffusion rate of released waste ions depends on the microstructural constitution referring to the mechanisms in diffusive transport and the sorption by the clay matrix of varying density. In general, diffusion refers to the transport of elements by action of random motions and works to eliminate distinct discontinuities in concentration. For smectite clay this process is complex since interlamellar diffusion is a 2-dimensional process on the microscale and takes place in diffuse electrical double-layers on the basal planes of the clay crystallites. This is in contrast with pore diffusion which is a 3-dimensional process. By making use of microstructural parameters one can distinguish the different contributions to bulk diffusion migration and create a basis for theoretical modelling of diffusive ion migration.

Keywords: Smectite clay, canisters, diffusion, montmorillonite, ion migration, clay microstructure.

---

[1] Lulea Technical University, Lulea, Sweden
[2] Ascend Technologies Ltd, Southampton, UK

Article Info: *Received:* June 5, 2019. *Revised:* August 23, 2019.

1. Introduction – Scope of study

The study was intended to show how one can describe conceptually and theoretically the rate of diffusive migration through smectite clay of single radionuclides escaping from failed canisters with highly radioactive waste (HLW). As with hydraulic conductivity, ion diffusion rate and mass transport can be estimated using microstructural parameters referring to 2D and 3D conditions.

Despite the stochastic nature of the particle network, implying considerable variations with respect to width and straightness of channels, as well as the density of clay gels filling them, F-parameters defined as in Figure 1 (Pusch and Yong, 2006) can be used for characterizing microstructural features depicted, by use of microscopy, stacks of smectite lamellae, stack aggregates and non-smectite grains in space (a), and gel-filled and unfilled voids in space (b).

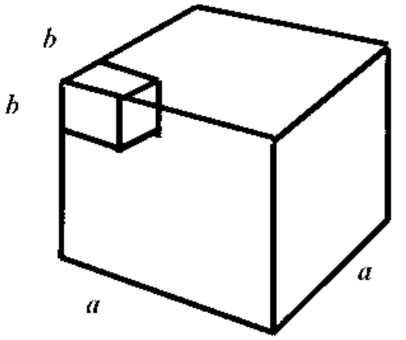

In 2D: $F_2=b^2/a^2$ $b=a(F_2)^{1/2}$

In 3D: $F_3=b^3/a^3$ $F_3=F_2(F_2)^{1/2}=(F_2)^{3/2}$ $\rho_{av}=\rho_b F_3+\rho_a(1-F_3)$

Figure 1: Way of defining microstructural features in 2D and 3D. ρ_{av} is the average bulk density of the whole clay element and ρ_a and ρ_b is the average density of components *a* (dense stacks of smectite lamellae, stack aggregates and non-smectite minerals) and of *b* (soft gel fillings and open space) (F_2 is a measure of Darcy permeability while F_3 is related to migration of dissolved matter in 3D).

Statistical analysis can be carried out of suitably defined and determined microstructural parameters F_2 and F_3, considering that the clay matrix consists of two components (Pusch and Yong, 2006): *a)* being medium to dense clay substance, and *b)* being soft to medium-dense clay substance, respectively. This distinction is made on the ground that *a* is completely or largely impermeable while *b* offers little or no flow resistance.

Relation of the microstructural parameter F_3 to migration of ions is more complex than the relation of function F_2 to permeation, since component *a* interacts by cation adsorption (K_d-effect) and hinders the movement of big molecules due to geometrical obstacles, therefore, they migrate both by pore and surface diffusion, while in the *b*-space ion migration is largely caused by pore diffusion. The two microstructural components are related through the coefficients F_2 for 2D and F_3 for 3D conditions. The ratio F_3/F_2 depends on the average and individual bulk densities as exemplified in Figure 2 for a commercial bentonite ("MX-80"). This procedure for density-related microstructural characterization can be applied to any soil analyzed with respect to the microstructural constitution using micrographs of very thin sections.

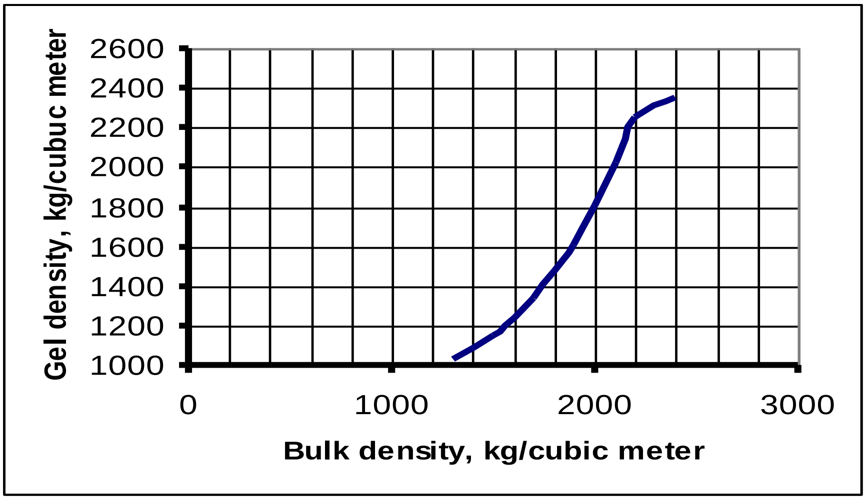

Figure 2: Correlation of the average gel density (ρ_g) and the average bulk density (ρ_{av}) for Wyoming bentonite (MX-80).

For any smectite clay the sum of the cross sectional area of individual voids identified in high-resolution micrographs, is used for relating it to the density and laboratory-determined hydraulic conductivity by considering the voids as sectioned channels serving as Poiseuille microtubes for deriving the F2 parameter, which is hence a measure of the permeable fraction of the micrograph section related to hydraulic conductivity and density. A simple and often sufficiently accurate way is to derive F2 from computer scanning of the micrographs. The obtained parameter values for F2 and F3 are unique for the clay in question. Considering the uncertainty in estimating interconnectivity and tortuosity of the gel-filled voids and channels, distinguishing only between permeable and impermeable fractions of the sections as a first order simplification, appears to be reasonable. F-data together with calculated and experimental K-values are shown in Tables 1 and 2 for three representative bulk densities, F3 being a measure of ion concentration per m3. Good agreement is obtained between the model-derived data for artificially prepared Wyoming clay (MX-80) in Na form and experimentally determined results.

Table 1: Microstructural data, conductivities in m/s, and cation concentrations for MX-80 in Na form (Pusch and Yong, 2006).

Bulk (total /dry) density [kg/m^3]	F_2/F_3	**Gel density (total/dry) [kg/m^3]**	**Experimental gel conductivity [m/s]**	**Calculated bulk conductivity [m/s]**	**Experimental bulk conductivity [m/s]**
2130/1794	0.17/0.07	2000/1590	7E-14	E-14	2E-14
1850/1349	0.24/0.12	1650/1030	2E-12	4E-13	3E-13
1570/904	0.40/0.26	1150/ 238)	2E-10	8E-11	8E-11

The microstructural heterogeneity of artificially prepared[3] MX-80 clay[4] is a significant factor especially for the hydraulic conductivity but also for the ion diffusivity of clay of this kind. In comparison to natural sedimentary clays with the same density and smectite content, the results indicate that higher hydraulic conductivity values are obtained for artificially prepared MX-80 clay since it maintains some of the natural granular form.

From the perspective of DDL interactions within the clay matrix, replacement of the original Na^+ by Ca^{2+}, Cd^{2+} and some radionuclides will raise the hydraulic conductivity. If one assumes the same F_2 values and gel densities as for MX-80 in Na form and uses typical gel hydraulic conductivities for MX-80 in Ca form, one obtains the results shown in Table 2. In the table, the bulk density of MX-80 in virgin form is given in the first column. The results shown in other columns refer to this clay in Ca form. As can be seen, good accord is obtained between calculated and true conductivity data except for the lowest bulk density, which is explained by microstructural heterogeneity caused by coagulation.

---

[3] Drying, crushing, sieving.

[4] Representative of smectite clays with 60-80 % montmorillonite

Table 2: Microstructural and conductivity data for MX-80 in Ca form. Percolation with strongly brackish Ca-dominated water according to Pusch and Yong, 2006.

Bulk density [kg/m^3]		***F_2***	**Gel density* [kg/m^3]**	**Gel conductivity [m/s]**	**Calculated bulk cond. [m/s]**	**Experimental bulk cond. [m/s]**
2130	Na	0.17	2000	2E-13	3E-14	3E-14
1850	Na	0.24	1650	8E-11	2E-12	2E-12
1570	Na	0.40	1150	7E-5	3E-06	2E-09
*Density at water saturation. Corresponding dry densities are 1590 kg/m^3 for the highest density, 1030 kg/m^3 for the intermediate density and 240 kg/m^3 for the lowest density.						

2. Mechanisms involved in ion diffusion-basics

We will first consider a theoretical model for diffusion of adsorbed spherical Brownian particles within the structure of a porous medium composed of zones of parallel planar surfaces representing aggregates of equally oriented smectite lamellae. The model worked out by Pusch, Muurinen, Lehikoinen, Bors and Eriksen (1992), implies differential flux of Brownian particles in a microscopic channel (the interlamellar space of less than 0.3 nm wide gap between adjacent stacks of lamellae) assuming local adsorption equilibria along the diffusion path. For the simple case of steady state transport with *G* taken as macroscopic concentration gradient, the electric field gradient induced by the negatively charged channel walls aligns dipolar particles and reduces their mobility by “electroviscous” effects. Traditionally, one distinguishes between pore diffusivity D_p, D_e (“effective” diffusivity), and D_a (“apparent diffusivity”). Here, we will use the first-mentioned**.** The authors used a microstructural model termed GMM, proposed by Pusch et al (1990), based on void size distributions evaluated from electron micrographs, according to Pusch and Yong, 2006; Bouchelaghem and Pusch, 2017), applying Hagen/Poiseuilles theory of water transmissivity of tubular systems. In principle, the microstructure was modelled as an array of non-interconnected parallel capillaries with periodic step changes in diameter for calculation of equilibrium ionic distributions within representative volumes (REV[5]) for three bulk densities as indicated in Table 3. Figure 3 shows a schematic picture of the GMM model with the grey bars representing smectite lamellae and the defined REV.

---

[5] Representative Elementary *Volume* for F_3 and Representative Elementary *Section* for F_2.

Table 3: Estimated channel dimensions (Pusch, 1999).

Bulk density (total/dry) [kg/m^3]	D1 [nm]	D2 [nm]	L1 [nm]	L2 [nm]
2130/1790	5	1	10	5
1850/1350	10	2	20	10
1570/905	50	3	100	50

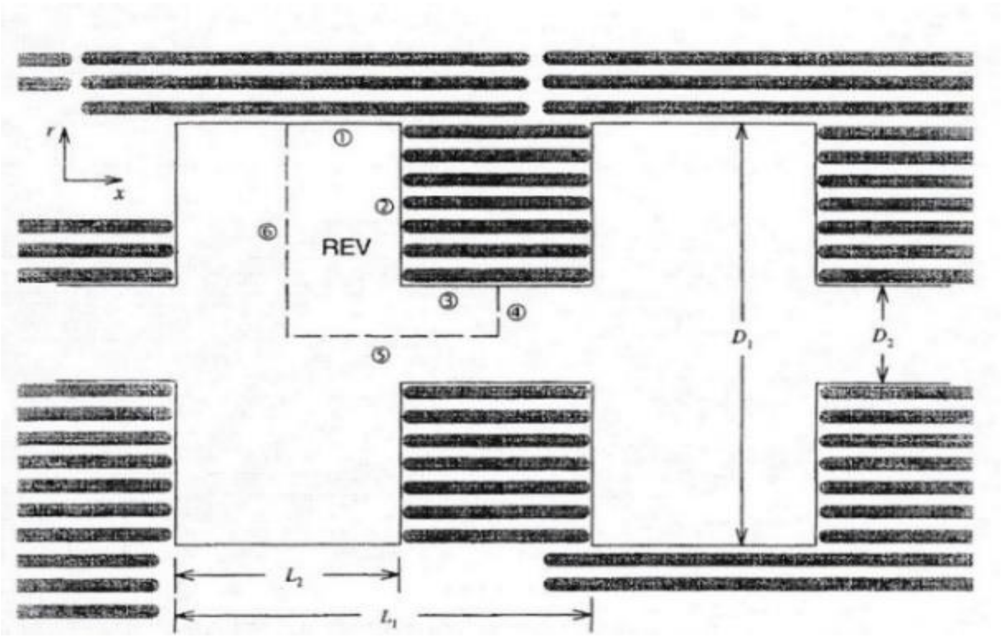

Figure 3. Ultrafine pore geometry of smectite clay.

The anion concentration in the REV for the listed high dry bulk density 1790 kg/m^3 calculated numerically as shown in Figure 4 is of particular importance since a density of this magnitude is aimed at for the clay surrounding canisters with high-level radioactive waste in a real repository (Svemar, 2005).

Determination of the porewater composition by chemical analysis only gives average values since the ions are not uniformly distributed in the clay matrix (Figure 4). Thus, the interlamellar porewater, which is free from anions, cannot be distinguished from the free porewater by such analyses but chemical modelling can be made based on microstructural models of the distribution of porewater. Expulsion of porewater under successively increased pressure gives a change in composition since low pressures expel water contained in large voids while high pressures cause migration of water from small voids and ultimately from the interlamellar space.

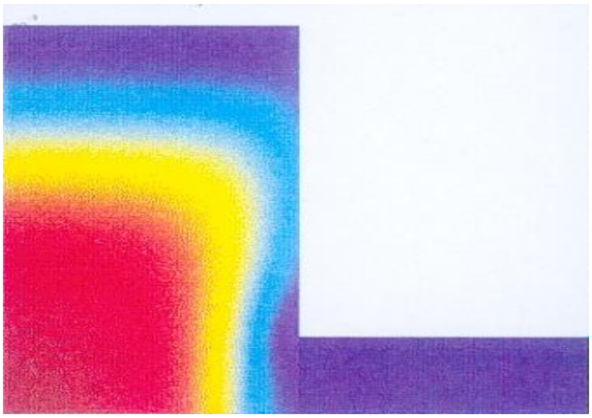

Figure 4: Distribution of ion concentration in the REV of Figure 3 at saturation with 0.1 M monovalent electrolyte of the microstructural network of MX-80 clay with dry density 1790 kg/m^3. Anions (red and yellow) are confined in the centers of the wide channels while cations (blue) are close to the negatively charged mineral surfaces (Pusch et al, 1999).

2.1 Microstructural constitution of MX-80 montmorillonite-rich clay

The factors controlling transport and fate of migrating contaminant ions are: (a) type and activity of clay substance, (b) cation exchange capacity (CEC) and specific surface area (SSA) of the soil solids, (c) chemistry of the porewater, (d) nature of species and concentrations of the contaminant ions, taken here to be radionuclides, (e) redox potential and pH. Everything else being equal, the migration rate of ion species in clay depends on the degree of sorption and the concentration gradients. Cation diffusion takes place in several ways, i.e. in continuous water-filled voids, along particle surfaces with electrical double-layers, and through the interlamellar space in smectites (Figure 5). The latter two mechanisms involve ion-exchange mechanisms for which the sorption parameter K_d, is used. In practice, the ion transport capacity can be predicted by applying Fick's law and relevant values of the coefficient of the density-related ”effective” diffusion, D_a.

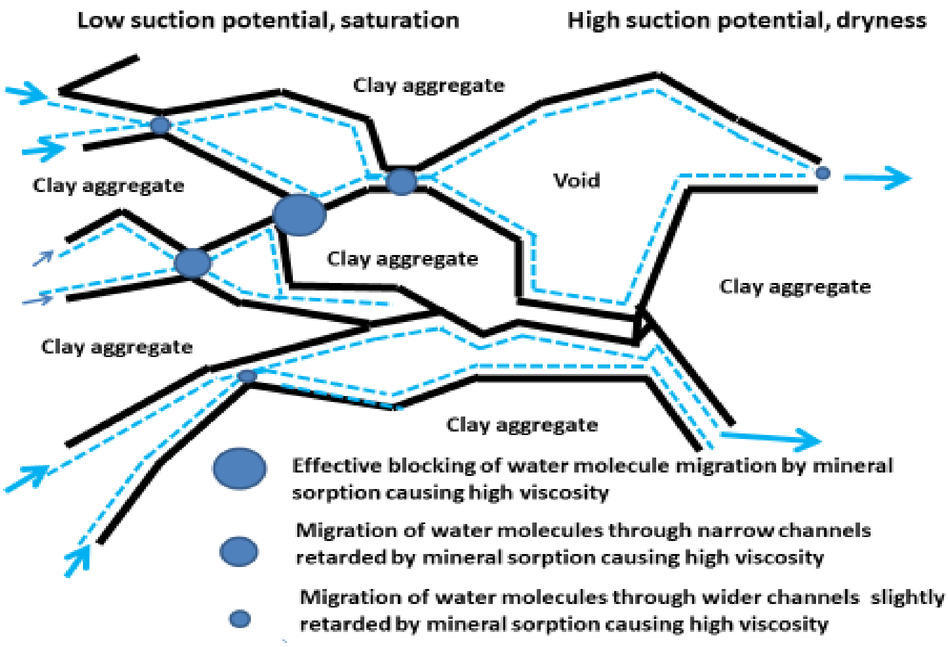

Figure 5: Migration of porewater in smectite element driven by a pressure or suction gradient.

Microscopic and submicroscopic channels in the clay matrix of artificially manufactured smectite clay are inherited from its initial granular constitution that is relatively unaffected by cyclic desiccation/rehydration of the clay, while wider channels undergo various changes in geometry and physical performance associated with water migration. The cross section of an element of water saturated smectite clay shows permeable channels that can be characterized with respect to shape and size by optical and electron microscopy, leading to the relationship of the density at water saturation as illustrated by the diagram and the schematic 2D microstructural model in Figure 6. The diagram indicates that the permeable fraction of a cross section and the water transport capacity are vanishingly small for densities at water saturation of more than 2100 kg/m^3.

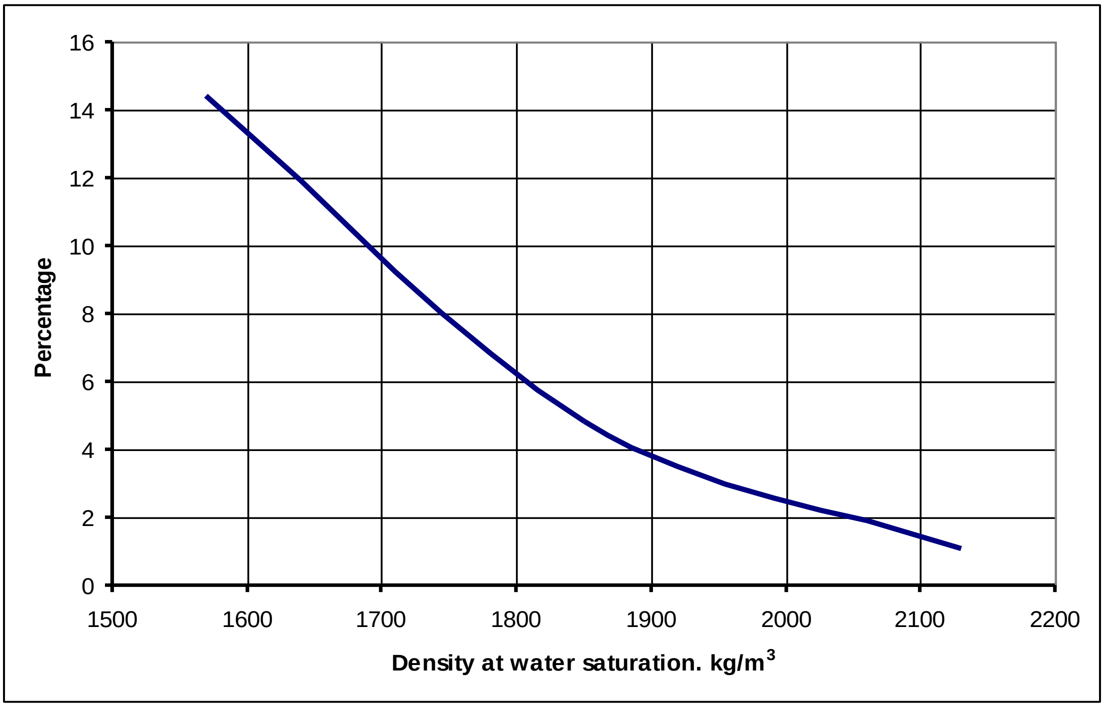

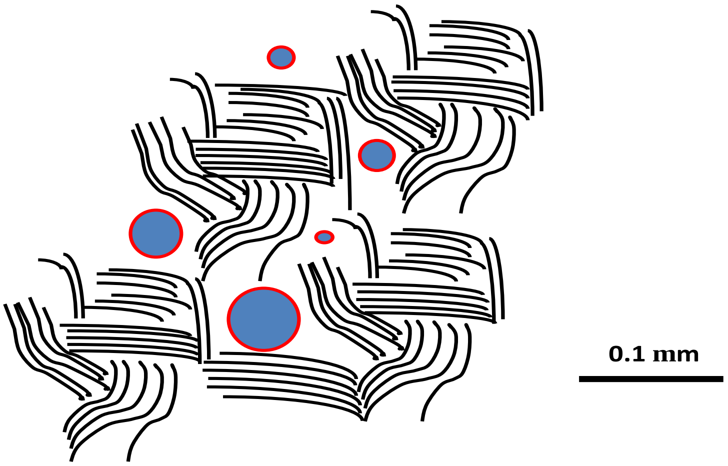

Figure 6. Channeling in smectite-rich clay prepared from compacted granules and percolated with fresh-water. Left: Channel cross section area as percent of total section area of smectite in Na form (Pusch, 2008).

Below: Schematic cross section of the microstructure (Pusch, 2015).

The space between lamellae is occupied by structured and highly viscous water coupled with cations or positively charges molecules. The coupling is strong for Ca and weak for Li and Na. The radionuclide transport through clay is a function of several factors; retardation is mainly by sorption and tortuosity. The process and values of migration parameters influence the radionuclide release, which are represented by geochemical interactions between the porewater and waste solidification matrix, and interactions among the chemical speciations of the water and the clay matrix. One distinguishes between the concentration of radionuclides on the solid phase (dry density basis) and their concentration in the liquid phase at equilibrium, which is affected by the distribution coefficient K_d (kg^{-1}) and the retardation factor $R=1+K_d \cdot \rho/n$, where ρ is dry density in kg/m^3, n is porosity (m^3/m^3), and K_d is the distribution coefficient in kg^{-1}. If the radionuclides have affinity to the clay element they are adsorbed and released from the porewater. The retardation factor R is also defined as R=Va/Vr, where Va is the rate of moved porewater (m/s) and Vr is the rate of migration of radionuclides in m/s.

Here, we will confine ourselves to consider the paths and spread of ions at steady state diffusion of positive and negative radionuclides through smectite clay assuming constant gradients in ion concentration. The mineral-degrading effect of α radiation has to be considered in detailed analysis of migration of positively charged radionuclides like plutonium and americium (Pusch et al, 1993; Beall, 1994), which can move in electrical double-layers and interlamellar space very close to smectite clay lattices as demonstrated by Figure 4.

2.2 Radionuclide diffusion

2.2.1 General

Smectite clay seals have low permeability, therefore, diffusive migration of radionuclides can be beneficial to their sealing function. The cation exchange capacity (CEC) determines the migration rate when the concentration of radionuclides is high, which is the case if a waste canister starts leaking. For the smectite family CEC can be taken as 100 meq/100 g (solid clay) meaning that a 0.5 m thick clay seal with a dry density of 1790 kg/m3 can bind approximately 895,000 meq per m^2. If Na is the dominant original cation it can be exchanged by positive radionuclides and when saturation has taken place the clay seal will let them through only by diffusion in absence of hydraulic gradients.

2.2.2 Applicability of microstructural parameters

As for hydraulic conductivity one can apply a simple way of visualizing the ion flux by utilizing the F2 parameter assuming 2D conditions and steady state conditions. For cations the flux is calculated as the rate of change of the mass concentration of radionuclides on the solid phase (a-space, dry density) by using the distribution coefficient Kd (kg-1) and a retardation factor R=1+Kd· ρ/n, where ρ is dry density in kg/m3 and n is porosity (m3/m3). For anions the ion flux can be taken as the change in mass concentration of radionuclides in the porewater, which dominates in soft gel fillings and open space (b-space in Figure 1), (cf. Table 4). Figure 7 exemplifies the distribution of electric potential and concentration of diffusing Sr cations according to Yang and Wang (2019).

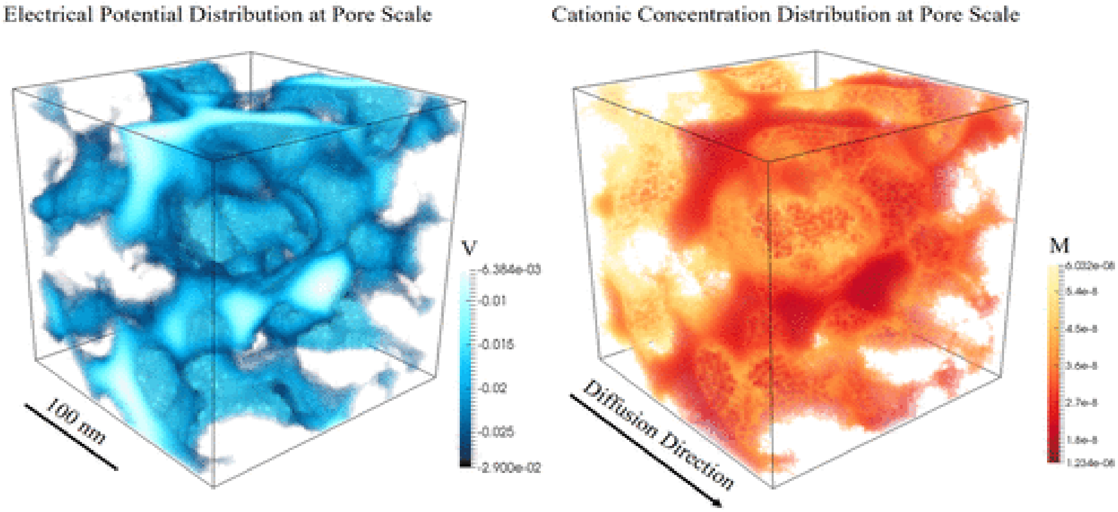

Figure 7. Electric potential and concentration of diffusing Sr ions in smectite (Yang and Wang, 2019).

Table 4: Ion concentration at saturation with the cation in question = Co, and microstructural and physical data for MX-80 with different dry densities (Pusch and Yong, 2006). Cation concentrations are evaluated from the product of F3, dry clay density and amount of meq of the dry clay mass (100 per g clay).

Total solid clay in *a*-space, kg/m^3	***F_2***	***F_3***	**Total water content in *b*-space [kg/m^3]**	**Mean cationic concentration at constant concentration gradient in a-space [kg/m^3]**	**Mean anionic concentration at constant concentration gradient in *b*-space [kg/m^3]**
1794	0.17	0.070	206	C_{oc} from start to C_{tc} etc[6]	C_{oa} from start to C_{ta} etc
1349	0.24	0.118	301	C_{oc} from start to C_{tc} etc	C_{oa} from start to C_{ta} etc
904	0.40	0.253	246	C_{oc} from start to C_{tc} etc	C_{oa} from start to C_{ta} etc
*Ctc and Cta denote concentrations of cations and anions at time t, respectively.					

As to the rate of diffusion one can consider cations and anions separately. We refer, as an example, to the divalent cation Cd and the monovalent anion Cl and calculate C_{tc} as indicated in Table 5. The F_3 parameter is best suited for dealing with the ion concentration of the assumed clay seal by using direct proportionality of C_{tc}, dry clay mass and F_3, assuming that the clay has been quickly saturated with Cd leachate. However, as we see from Figure 7, the concentration of cations is not uniform over the cross section, which requires definition and use of an "effective" fraction of the total cross section for calculating the distribution of Cd ions over a cross section area represented by F_2.

One finds as an example that if the leakage of Cd from contacting radioactive waste in liquid form is constantly E-6 mg/l, the densest clay seal with 0.5 m^3 volume and 897 kg dry clay will take up about 89,700 meq of Cd, and ultimately give the clay seal a Cd content of about 90 ppm. The large part of it is successively transferred to the surroundings since the clay will be early saturated with this cation (cf. Kandah et al, 2010).

The diffusive anion transport capacity is proportional to the ratio of the pore space between the stacks of smectite lamellae and the total pore space, the anions being excluded from the interlamellar space by the Donnan effect. At increasing density there is strong reduction of the available space for migration, and the diffusion coefficient of anions therefore drops significantly. Since many cations move both by pore and surface diffusion, the retarding effect resulting from increased density on the diffusion capacity of cations is limited. Table 6 summarizes the mean concentration of Cl in the porewater of the clay seal at equilibrium. In our example the ratio of cation and anion concentration (90/57 ppm) is 1.58. This is assumed to represent also the ratio of cation and anion diffusion coefficients.

Table 5: Mean concentration of radioactive cadmium in 0.5 m thick clay seal with 1 m^2 cross section area in contact with Cd-leaking waste container.

Solid clay mass (*m*) in *a*-space, [kg/m^3] (dry density)	**Mean Cd concentration under steady state conditions in *a*-space**
1794 F_3=0.070	C = 2510 mg/l (ppm)
1349 F_3=0.118	C = 530 mg/l (ppm)
904 F_3=0.255	C = 457 mg/l (ppm)

Table 6: Mean anion concentration (C) in 0.5 m thick clay seal with 1 m^2 cross section area in contact with steady-state leaking waste container giving off monovalent anions at equilibrium.

Water content in *b*-space [kg/m^3]	**Controlling parameter F_3**	**Mean anionic concentration in *b*-space [ppm]**
206	0.07	C = 0.07x206 = 14.4 ppm
301	0.118	C = 0.118x301= 35.5 ppm
246	0.255	C = 0.255x246= 62.7 ppm

The EPA regulations of USA imply a maximum allowed concentration of radionuclides in public drinking water of 30 μg per liter, i.e. 3E-9 mg/l =3E-9 ppm. For our densest case of a clay seal percolated by seawater with contaminant Cd cations, the mean anion (Cl) concentration in the porewater of the clay seal, with 206 kg total amount of porewater, would reach about 14 ppm. The Cd concentration of the heavily charged solid clay phase, saturated with this ion, would be 2510 ppm, according to the calculations.

3. Experimental

Everything else being equal, the transport rate of ion species in clays depends on their diffusivity and concentration gradients. The diffusion transport capacity in terms of the ”effective” diffusion coefficient refers to the actual ”effective” porosity and describes ion transport on the microstructural level. This is in contrast to the ”apparent” diffusion coefficient, which is a general measure of diffusion derived directly from recorded concentration profiles. As mentioned, cation diffusion takes place in several ways, i.e. in continuous water-filled voids, along particle surfaces with electrical double-layers, and through the interlamellar space in smectites.

The latter two mechanisms involve ion-exchange mechanisms for which the sorption parameter, K_d, is responsible. As the calculations demonstrate, the ion transport capacity is largely controlled by the dry density which is indicated by various published experiments like the ones leading to the results in Figure 8. The ratio of the cation and anion diffusivities in Kato’s experiments varied between 5 and more than 150 while the present study indicates a ratio ranging between 7 and 15 for medium dense clay, which is in reasonable agreement with data for diffusion coefficients published by Roehl and Czurda (2019), i.e. 4.9-6.7E-12 m^2/s.

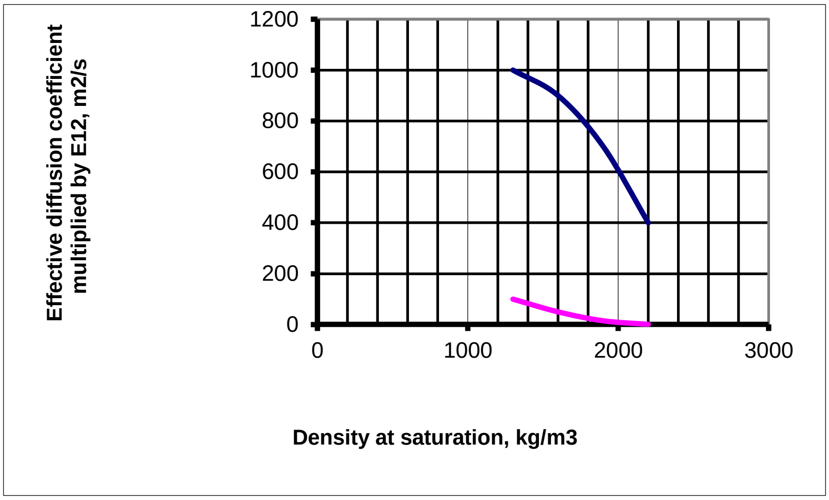

Figure 8. Measured effective diffusivities for smectite clay (Kato et al,1995). Upper: monovalent cations. Lower: monovalent anions like chlorine.

4. Comments and discussion

Microstructural parameters F_2 and F_3 can be used for distinguishing between the different contributions to bulk diffusion and for creating a basis for theoretical modelling of diffusive ion migration. The major findings reported in the paper are the following:

- F_2 and F_3 can be evaluated from digitalized TEM micrographs with different degrees of greyness representing different densities. They can be converted into different colours for easy interpretation and representation of the variation of density. Good correlation has been found between these parameters and physical properties like hydraulic conductivity and expandability in terms of swelling pressure (Pusch and Yong, 2006; Bouchelaghem and Pusch, 2017).

- Since the F_2 parameter represents the part of the clay in which pore diffusion dominates, it determines the diffusive capacity of anions and molecules. Thus, the ratio of the void volume available for uniaxial diffusion and the total volume should be approximately proportional to F_2 for cations, and proportional to unity for lithium and sodium. The ion diffusion coefficient for e.g. iodine and sodium should be about E-10 m^2/s for a bulk density of 2000 kg/m^3, which is about 4 times higher than published experimental data (Brandberg et al, 1991; Pusch et al, 1999). The main reason for this discrepancy is that channel tortuosity and constrictions have not been accounted for in the model.

- The diffusive anion transport capacity is proportional to the ratio of the space of the voids between the stacks of smectite lamellae since they are excluded from the interlamellar space by the Donnan effect. With increasing density there is strong reduction of the available space for migration, and the diffusion coefficient of anions therefore drops significantly. Since many cations move both by pore diffusion and surface diffusion, the retarding effect on the diffusion capacity of cations resulting from increased clay bulk density is limited, especially for monovalent ions.

- Since the F_2 parameter represents the water-rich part of the clay in which pore diffusion takes place, it determines the diffusive capacity of most ions and molecules. Thus, the ratio of the void volume available for uniaxial diffusion and the total volume should be approximately proportional to F_2 for anions, and to unity for lithium and sodium. The ratio of the ion diffusion capacity of iodine and sodium, and monovalent anions should be about 6 for a bulk density of 2000 kg/m^3. This is about 4 times higher than reported experimental ratios. The main reason for this discrepancy is that channel tortuosity and constrictions have not been accounted for in the model used.

- Since F_2 is density-dependent it is expected that prediction of ion fluxes using this parameter value would show a clear drop for anions with increasing clay density since anions are prevented from entering interlamellar space by Donnan exclusion. Cations on the other hand would not be as much affected by an increase in clay density. This is also demonstrated by the results from which one would be tempted to conclude that one should strive to obtain very high clay seal densities in practice. However, there is a price to pay, which is the problem of very high swelling pressures, since it can cause displacement and failure of supporting constructions in repositories.

References

[1] Beall, G.W. (1984). The implications of alpha radiation damage for bentonites utilized in high-level waste disposal. Smectite Alteration. Swedish Nuclear Fel and Waste Management (SKB) Technical Report TR 84-11.

[2] Bouchelaghem, F and Pusch, R. (2017). Fluid flow and effective conductivity calculations on numerical images of bentonite microstructure. Applied Clay Science, 144, 9-18.

[3] Brandberg, F. and Skagius, K. (1991). Porosity, Sorption and Diffusivity Data compiled for the SKB 91 Study. Swedish Nuclear Fel and Waste Management (SKB) Technical Report TR 91-16.

[4] Darban, A.K. (1997). Multi-component transport of heavy metals in clay barriers, PhD thesis, McGill University.

[5] Kato, H., Muroi, M., Yamada, N., Ishida, H. and Sato, H. (1995). Estimation of the effective diffusivity in compacted bentonite. In: Scientific Basis for Nuclear Waste Management XVIII. Mat. Res. Soc. Symp. Proc., Vol. 353, MRS, Pittsburg, USA.

[6] Kandah, M.I., Abu Al-Rub, F., Bawarish, L., Bawarish, M., Khalil, H. Al Reem and Saada, R. (2010). Afsorption of Cadmium onto Activated, Non-activated Date Pits. World Academy of Science and Technology, 62.

[7] Osipov, V.I., Sokolov, V.N. and Eremeev, V.V (2004). Clay seals of oil and gas deposits. A A Balkema Publishers, Lisse/Atingdon/Exton (PA)/Tokyp ISBN 90 5809 90 5809 583 5.

[8] Pusch, R., Karnland, O. and Hökmark, H. (1990). GMM-A general microstructural model for qualitative and quantitative studies of smectite clays. Swedish Nuclear Fuel and Waste Management AB (SKB). Technical Report TR 90-43, SKB Stockholm.

[9] Pusch, R., Karnland, O., Lajudie, A. and Decarreau, A. (1993). MX-80 clay exposed to high temperatures and gamma radiation. Swedish Nuclear Fuel and Waste Management AB (SKB). Technical Report TR 93-03, SKB Stockholm.

[10] Pusch, R. (1998). Transport of radionuclides in smectite clay. In: Environmental Interaction of Clays, Eds. A. Parker and J.E. Rae. Springer Verlag, Berlin-Hedielberg (ISBN: 3-540.58738-1).

[11] Pusch, R. (1999). Experience from preparation and investigation of clay microstructure. Engineering Geology, 54 (187-194).
[12] Pusch, R., Muurinen, A., Lehikoinen, J., Bors, J. and Eriksen, T. (1999). Microstructural and chemical parameters of bentonite as determinants of waste isolation efficiency. Final Report, European Commission Contract No F14W-CT95-0012.
[13] Pusch, R. and Yong, R.N. (2006). Microstructure of Smectite Clays and Engineering Performance. Spon Research, Taylor & Francis, New York.
[14] Roehl, K.E. and Czurda, K. (2019). Diffusion and solid specification of Cd and Pb in clay liners, ScienceDirect.
[15] Yang, Y. and Wang, M. (2019). Cation diffusion in compacted clay: A pore-scale view. Environmental Sci. Technology, 53(4), 1976-1968.
[16] Yong, R. N. (2003). Influence of microstructural features on water, ion diffusion and transport in clay soils. Journal of Applied Clay Science, 23 (3-13).